Hawiger, J., Parksinson, S., & Timmons, S. (1980) *Nature (London) 283*, 195–197.
Kahn, C. R. (1975) *Methods Membr. Biol. 3*, 81.
Kekwick, R. A., McKay, M. E., Nance, M. H., & Record, B. R. (1955) *Biochem. J. 60*, 671–683.
Marguerie, G. A., Plow, E. F., & Edgington, T. S. (1979) *J. Biol. Chem. 254*, 5357–5363.
Marguerie, G. A., Edgington, T. S., & Plow, E. F. (1980) *J. Biol. Chem. 255*, 154–161.
Mihalyi, E. (1968) *Biochemistry 7*, 208–223.
Mustard, J. F., & Packham, M. A. (1970) *Pharmacol. Rev. 22*, 97–187.
Mustard, J. F., Packham, M. A., Kinlough-Rathbone, R. L., Perry, D. W., & Regoeczi, E. (1978) *Blood 52*, 453–466.
Niewiarowski, S., Morinelli, T., & Budzynski, A. Z. (1980) *Fed. Proc., Fed. Am. Soc. Exp. Biol. 39*, 543.
Peerschke, E. I., Zucker, M. B., Grant, R. A., Egan, J. J., & Johnson, M. M. (1980) *Blood 55*, 841–847.
Praga, C. A., & Pogliani, E. M. (1973) *Thromb. Diath. Haemorrh. 29*, 183–189.
Singer, S. J. (1974) *Annu. Rev. Biochem. 43*, 805–833.
Vignais, P. M. (1976) in *Mitochondria, Bioenergetics, Biogenesis, and Membrane Structure* (Packer, L., Ed.) pp 367–379, Academic Press, New York.

Spectral Evidence for a Rapidly Formed Structural Intermediate in the Refolding Kinetics of Hen Egg-White Lysozyme†

Shingo Kato,‡ Motoyoshi Okamura, Nobuo Shimamoto, and Hiroyasu Utiyama*

ABSTRACT: For investigation of the conformation of the unfolded species and its role in the refolding kinetics, refolding kinetic measurements were made on hen egg-white lysozyme by using the stopped-flow method at 25 °C in the four sets of initial and final folding condition: (1) 4 M guanidinium chloride (GdmCl) and 0.5 M GdmCl; (2) 40% acetic acid (HOAc) and 5% HOAc; (3) 4 M GdmCl and 0.5 M GdmCl–5% HOAc; (4) 40% HOAc and 0.5 M GdmCl–5% HOAc. The kinetic results as measured by absorbance at three wavelengths, 301, 292, and 250 nm, agreed with each other and indicated strict biphasic behavior without exception. The kinetic parameters were determined only by the final refolding conditions. The spectral properties of the unfolded species at the end of stopped-flow mixing were investigated by comparing the total kinetic amplitude with the difference between the static absorbance of the native molecule in the final refolding conditions and that of the unfolded molecule in the initial unfolding conditions. The solvent effect was considered in the comparison. It was concluded that the unfolded species assumed a new transient conformation in the mixing process and that the transformation was completed within the mixing time.

In kinetic studies of the refolding of small proteins stopped-flow technique is often used, where the denatured protein solution is quickly brought to the refolding condition by mixing with some diluent and the refolding process taking place thereafter is followed by spectral measurements. The most extensive investigation was made by the Baldwin group on bovine pancreatic ribonuclease A (RNase A)[1] [review by Baldwin (1975, 1978)]. It was shown that, in the direct folding reaction (folding of the fast-folding form), the small protein refolded from the denatured and extended conformation into the native and compact one essentially in a single kinetic process. This result indicates that the refolding process involves highly cooperative interactions among many parts of the molecule. The refolding rate, ranging from 10 to 100 s^{-1}, is therefore probably much slower than the rates of local conformational changes. The regular secondary structure is also formed more rapidly. The rate of α-helix formation in synthetic homopolymers ranges from 10^7 to 10^8 sec^{-1} (Schwarz, 1965; Hammes & Roberts, 1969).

In this paper we focus our attention on the conformation of the unfolded protein, by means of stopped-flow refolding studies. The above discussion suggests that, when unfolded molecules start folding within the mixing process of the stopped-flow apparatus, the molecules may acquire, at the end of mixing, a new local secondary structure different from the one in the initial unfolding conditions. The unfolded molecule with the new secondary structure would exist only transiently as a refolding intermediate, and the new local secondary structure would be characterized by the refolding condition and might be the principal factor determining the refolding rate. If this is correct, the refolding kinetics should be determined solely by the final refolding condition, independent of the initial unfolding condition. The first purpose of this study is to show by spectral data that the unfolded conformation in refolding condition is different from that in the initial unfolding condition.

The second purpose concerns the refolding kinetics of hen egg-white lysozyme (HEWL). The three-species model $U_1 \rightleftharpoons U_2 \rightleftharpoons N$ (N = native, U_1, U_2 = unfolded) has been well established for the refolding process of RNase A (Garel & Baldwin, 1973, 1975a,b; Hagerman & Baldwin, 1976; Nall et al., 1978). It is not established, however, that the model is valid for other globular proteins. Even for HEWL, which has been widely used in physical studies of proteins, some experimental results now available (Tanford et al., 1973) are in apparent contradiction to the model: (1) the unfolding

† From the Life Science Group, Faculty of Integrated Arts and Sciences, Hiroshima University, Hiroshima 730, Japan. *Received June 6, 1980.* This work was supported in part by Research Grants B247134 and C458122 to H.U. from the Ministry of Education, Science and Culture of Japan.

‡ Permanent address: Institute for Chemical Research, Kyoto University, Uji 611, Japan.

[1] Abbreviations used: RNase A, bovine pancreatic ribonuclease A with disulfide bonds intact; HEWL, hen egg-white lysozyme with the intact disulfide bonds; GdmCl, guanidinium chloride; HOAc, acetic acid.

0006-2960/81/0420-1080$01.25/0

kinetics outside the transition zone are biphasic, and the amplitude of the fast phase increases with GdmCl concentration; (2) the refolding kinetic results at 292 nm do not display any biphasic character in contrast to the data obtained at 301 nm. In spite of these difficulties, it was pointed out (Hagerman & Baldwin, 1976; Hagerman, 1977) that the original data can be reconciled with the three-species model. In any case, however, the above contradiction should be resolved by the experimental data. We therefore investigated the refolding kinetics of HEWL in this study.

Guanidinium chloride (GdmCl) was used as a denaturing reagent as in other kinetic studies. This reagent is useful in that the folding transition is reversible without the interference of aggregation reactions. In the present study we introduced acetic acid (HOAc) as another denaturant. This reagent not only satisfies the above criterion as a useful denaturant but also differs substantially from GdmCl in its action as a denaturant. GdmCl is well-known as the denaturant that most effectively breaks the secondary structure. In contrast, lysozyme molecules undergo in equilibrium two cooperative transitions successively by the addition of HOAc, each to a β-like conformation (S. Kato et al., unpublished results). By using HOAc, therefore, we can design an interesting experiment in which the protein molecules initially denatured with either GdmCl or HOAc are refolded in the same refolding conditions containing both denaturant. Thus we may test whether the refolding kinetics are independent of the initial unfolded conformation.

Experimental Procedures

Materials. Hen egg-white lysozyme, grade I, was obtained from Sigma as three times crystallized, dialyzed, and lyophilized powder. It was subjected to a fractional precipitation with ammonium sulfate according to the method of Sophianopoulos et al. (1962). The purified sample was dialyzed against water and lyophilized. The sample thus prepared migrated as a single band in polyacrylamide gel electrophoresis in the presence and absence of $NaDodSO_4$. The gel systems were prepared with the solutions (a) 5% acrylamide, 0.14% *N,N'*-methylenebis(acrylamide), 0.1 M sodium phosphate buffer, pH 7.2, and 0.1% $NaDodSO_4$, and (b) 5% acrylamide, 0.14% *N,N'*-methylenebis(acrylamide), and 0.1 M Tris-HCl buffer, pH 8.0. Protein concentration was determined spectrometrically on the basis of $A_{280}^{1\%} = 26.3$ in 0.1 N HOAc (Wetlaufer et al., 1974). Special grade GdmCl for biochemical use was purchased from Wako Chemical Industries and its concentration was determined by the refractive index measurement (Nozaki, 1972). HOAc was guaranteed reagent grade from Nakarai Chemicals, Kyoto.

Stopped-Flow Measurements. The folding kinetics of HEWL were measured by using a stopped-flow spectrophotometer, Model RA-401 (Union Giken Company, Osaka). Denatured protein solution and diluent, thermostated separately in two reservoirs, were driven pneumatically, at about 5 kg/cm^2 pressure of nitrogen gas, through two serially connected four-jet mixers. A thermostated flow cell of 10-mm path length was used for spectral measurements. In order to mix unequal volumes of protein solution and diluent, we introduced a constriction in the flow channel from the reservoir of protein solution to the mixer. The constriction consisted of a Teflon gasket containing a small circular Teflon plate 2 mm thick with a pin hole whose diameter can be selected in the range 0.1–0.6 mm. The dilution ratio was determined from the protein concentrations before and after mixing, the value for the highest dilution being 35. In finely adjusting the denaturant concentration after the mixing to a preset value, an appropriate amount of denaturant was added to diluent. The use of two serial mixers was found necessary for the complete mixing of two liquids of extremely different volumes and concentrations. The dead time of the apparatus was determined as 20 ms from the measured rate of the pseudo-first-order reducing reaction of 2,6-dichlorophenol-indophenol sodium with L-ascorbic acid (Hiromi et al., 1968; Tonomura et al., 1978).

Monochromatic light with a band pass of 1.4 nm was obtained by using a combination of a 25-W deuterium lamp and a grating monochromator of the Czerny–Turner type. The beam was focused at the cell center and received by a photomultiplier tube (Hamamatsu R374) of a head-on type. The output signal, amplified so that unit absorbance corresponds to 1.00 V, was fed to a Union Giken 77 microcomputer for the data storage, averaging, and further analyses. The results were displayed on a X-Y recorder and stored in magnetic tape, if necessary. Since the refolding of lysozyme exhibited biphasic kinetics, the measurements in the short and long time ranges, each containing 250 data points, were carried out separately in one mixing. Acquisition of the data in the long time range was started at a preset time after the last measurement in the short time range had been completed. The sampling period could be changed stepwise in the range 20 ms–100 s per 250 points. Five single transients were averaged, and the result was analyzed by fitting it to sum of two exponential terms by the standard method of resolving two exponentials:

$$A - A_{eq} = A_1 \exp(-t/\tau_1) + A_2 \exp(-t/\tau_2)$$

The equilibrium value A_{eq} was first evaluated from the data of the long time range as an average of the data in the period longer than 6–7 times the characteristic time of the slower phase τ_1. The amplitude A_1 and the characteristic time τ_1 for the slower phase were determined from the linear region in the plot of log $(A-A_{eq})$ vs. time. The contribution of the slower phase evaluated in this way was subtracted from $(A-A_{eq})$ to determine the constants for the faster phase, A_2 and τ_2. In least-squares fits of absorbance data to a first-order plot, we used a weighting factor of $(A-A_\infty)^2$, where A_∞ denotes the absorbance when the respective relaxation was completed. The amplitude was expressed in molar absorbance on the basis of the molecular weight of 14314 (Canfield & Liu, 1965).

In order to compare directly the total amplitude of the kinetic measurement with the difference absorbance of the static measurement, we measured the difference in absorbance between the initial denatured protein solution and that of the native protein, in the final refolding conditions, in the same stopped-flow spectrophotometer. The two solutions, having been separately thermostated in two reservoirs, were driven to the cell one at a time by using a tiny plastic stopcock with a T shape. The apparatus was stable enough for quick pairwise measurements.

Denatured protein solutions were prepared with much care to avoid aggregated particles. The lyophilized sample was first dissolved in distilled water to a concentration of 50 mg/mL. The solution was then centrifuged at 4000*g* for 30 min, and the supernatant was filtered through a G2 glass filter. In preparing a denatured protein solution, the protein solution thus prepared was mixed with concentrated denaturant solution in an appropriate volume ratio and kept for certain time (1 h for GdmCl-induced denaturation and 10 min for HOAc-induced denaturation) for complete denaturation. The solution was filtered again through a G2 glass filter and used for stopped-flow measurements. Prolonged standing of protein in the denatured state, in HOAc systems in particular, was avoided. The absence of aggregates in the cell was checked

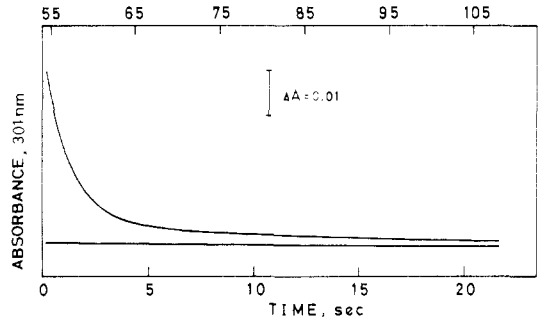

FIGURE 1: Kinetic progress curves for HEWL folding at 25 °C as measured by absorbance at 301 nm after a stopped-flow concentration jump from 4.0 M to 0.5 M GdmCl in 0.05 M glycine–HCl buffer, pH 2.6. The final protein concentration was 0.4 mg/mL. The upper and lower traces show the changes over the time ranges 0–20 s (lower abscissa scale) and 50–100 s (upper abscissa scale), respectively. The equilibrium value was obtained as an average of the data in the period longer than 90 s.

by measuring the absorbance at 340 nm, which is due to scattering. Two or three flushings of the flow channel were necessary for obtaining reproducible data.

The initial unfolding condition employed in this study was either 4 M GdmCl, pH 2.5, or 40% HOAc, pH 1.8. The final refolding conditions corresponding to these initial conditions were 0.5 M GdmCl, pH 2.6, and 5% HOAc, pH 2.6, respectively. Another refolding condition of 0.5 M GdmCl and 5% HOAc, pH 2.4, was also used. Except for the systems containing only HOAc, glycine–HCl buffer, pH 2.6, was added to 0.05 M. The temperature change on diluting the concentrated GdmCl solution was confirmed less than 0.1 °C from the absorbance change of phenolphthalein measured at 552 nm in glycine–HCl buffer, pH 8.8. No absorbance change was obseved at any wavelength by simple dilution of 4 M GdmCl solution with aqueous buffer. A Corning Model 12 pH meter was used to measure the pH of solutions before and after the mixing.

Difference Absorbance Measurements. Difference UV absorbance spectra were measured in a Hitachi 320 recording spectrophotometer equipped with a grating double monochromator of 0.07-nm resolution. A very low level of stray light, less than 0.0001%, and the use of differential feedback control of dynode voltage make this instrument suitable for difference absorbance measurements on protein solutions of high concentration. The gain for the servomechanism controlling the slit width was chosen high enough to obtain data independent of the setting. A pair of tandem quartz cells whose temperature was controlled at 25.0 °C by circulating thermostated water in the holder was used. Wavelengths were scanned in the range from 340 to 240 nm at a speed of 20 nm/min.

Results

Refolding Kinetics of Lysozyme Are Biphasic in Refolding Conditions Which Contain either 0.5 M GdmCl or 5% HOAc or Both. Figure 1 shows kinetic progress curves for HEWL folding at 25 °C as measured by tryptophan absorbance at 301 nm. The final refolding condition was 0.5 M GdmCl and 0.05 M glycine–HCl buffer, pH 2.6. It is seen that the trace in the long time range is smooth and approaches a constant value. The equilibrium value was determined as an average of the data at times longer than 90 s. The net absorbance change calculated by using the equilibrium value is plotted semilogarithmically in Figure 2 (the upper trace) to estimate the characteristic time and the amplitude for the slowest phase. The data at times longer than 10 s fall on a straight line nicely

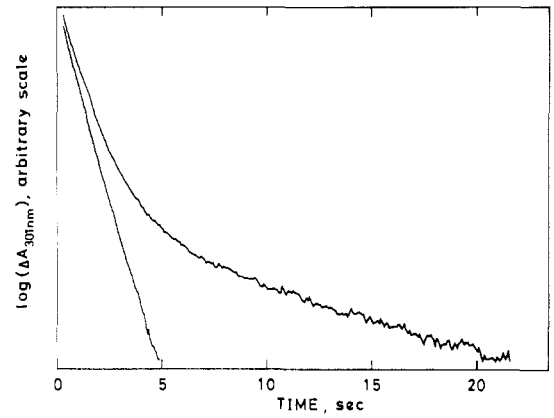

FIGURE 2: Semilogarithmic plots of the net absorbance change calculated from the data shown in Figure 1. The upper trace shows the whole change. The amplitude and the characteristic time for the slowest phase were evaluated by fitting the data longer than 10 s to a straight line by the method of least squares. The lower trace shows the residue obtained by subtracting the contribution of the slowest phase from the whole change.

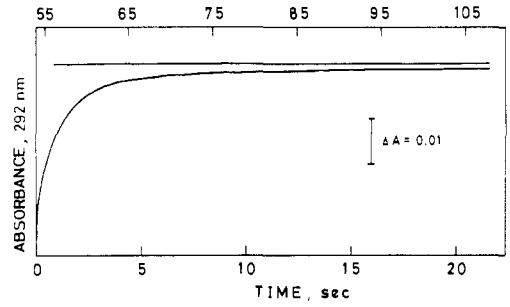

FIGURE 3: Kinetic progress curves for HEWL folding at 25 °C as measured by absorbance at 292 nm. For conditions, see the legend to Figure 1.

enough to be regarded as exhibiting a single phase. For unambiguously determining the numerical parameters for this phase, we definitely require measurements of high precision as well as averaging and processing data with the use of a microcomputer, because the amplitude of this phase is very small. The plots of the first residue after subtracting the contribution of the slowest phase from the total change (lower trace in Figure 2) already fall on a straight line. Thus we can safely conclude that the kinetics are biphasic: the residue after subtracting the contributions of the two relaxation processes from the whole change was checked to be small and within the experimental error.

The result of a similar experiment measured by absorbance at 292 nm is very interesting, since uniphasic behavior was reported previously. We obtained the biphasic behavior shown in Figure 3. The absorbance was increasing in this case during refolding. The biphasic behavior is more clearly seen in the semilogarithmic plot (Figure 4). Similar biphasic refolding kinetics were obtained by measurements at still another wavelength, 250 nm. Furthermore, all measurements, using different sets of initial and final conditions, yielded biphasic behavior without any exception in the present study.

Kinetic Parameters Are Independent of Wavelength and of the Initial Unfolding Condition. Table I summarizes the results for the characteristic times τ_1 and τ_2 and the amplitudes A_1 and A_2 of the two phases as well as the fraction of the fast phase in the total amplitude for the four sets of initial and final conditions. We note that the measurements at the three wavelengths give the same kinetic result. Scattering among the values of τ_1 is expected since the amplitude of the solwer phase is very small.

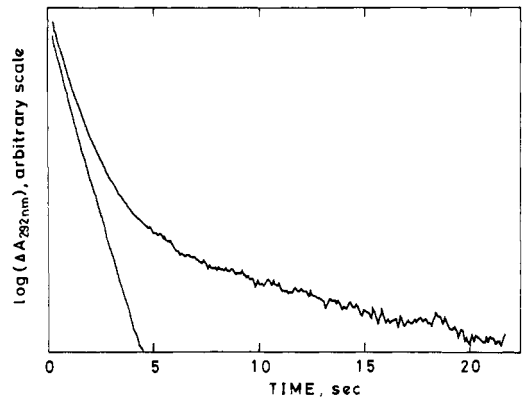

FIGURE 4: Semilogarithmic plots of the net absorbance change calculated from the data shown in Figure 3. For details, see the legend to Figure 2.

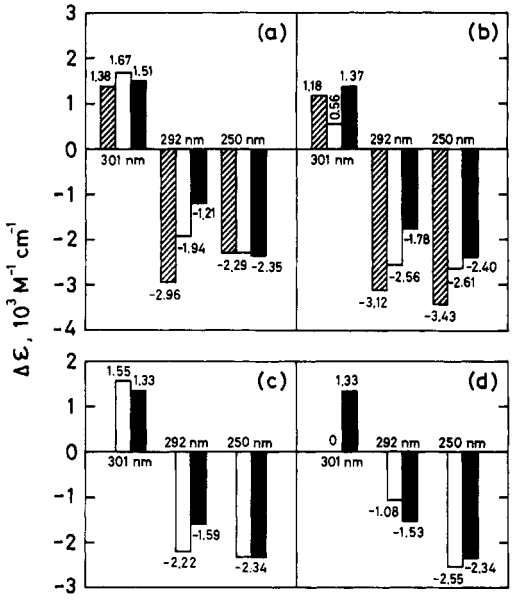

FIGURE 5: Comparison between the total kinetic amplitude (filled bars) and the absorbance difference between the initial unfolded protein and the native protein in the final refolding condition (open bars). The latter was obtained statically in the stopped-flow spectrophotometer at 25 °C. The hatched bars represent the static data corrected for the solvent effect (see the text). The denaturant concentrations used in the comparison were (a) 4 M and 0.5 M GdmCl, (b) 40% and 5% HOAc, (c) 4 M GdmCl and 0.5 M GdmCl–5% HOAc, (d) 40% HOAc and 0.5 M GdmCl–5% HOAc. The final protein concentration was 0.4 mg/mL. The 4 M and 0.5 M GdmCl solutions contained 0.05 M glycine-HCl buffer, pH 2.6.

It is interesting to note that the refolding of HEWL in 5% HOAc (final) is much faster than in 0.5 M GdmCl (final): eight times for the fast phase and five times for the slow phase. However, the fraction of the fast phase in the total amplitude is similar for both final conditions.

In the other two series of measurements, the stopped-flow jumps were made to the same final conditions (0.5 M GdmCl and 5% HOAc) from different initial conditions, either 4 M GdmCl or 40% HOAc. The use of mixed denaturants in the final condition allows us to test whether the refolding kinetic behavior is independent of the initial unfolding condition. The results (Table I) clearly show that the kinetic parameters for the two series of measurements agree with each other.

The presence of both denaturants in the refolding condition seems to retard the rates of both phases, 2-fold for the fast phase and 1.2-fold for the slow phase, in comparison to the data for 0.5 M GdmCl. The fraction of the fast phase in the total amplitude, 0.85 on the average, is significantly smaller than the value 0.90–0.92 for the other two refolding conditions.

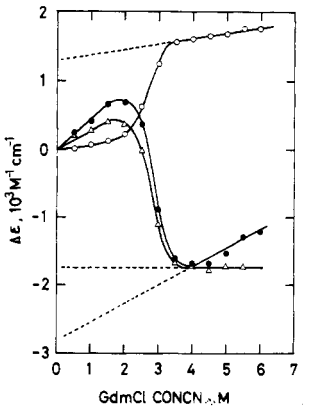

FIGURE 6: Change in molar absorbance of HEWL with GdmCl concentration at 25 °C, observed at 301 (open circles), 292 (filled circles), and 250 nm (triangles). The dotted line represents the linear extrapolation of the data in the post-transition region to the refolding condition. The measurements were made in a Hitachi 320 recording spectrophotometer.

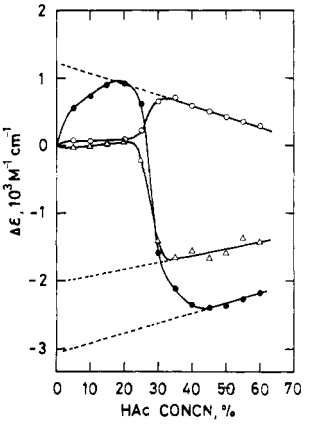

FIGURE 7: Change in molar absorbance of HEWL with HOAc concentration at 25 °C. See the legend to Figure 6 for the symbols.

Total Kinetic Amplitude Obtained in Refolding Differs from the Static Absorbance Difference between Unfolded and Native Protein. We show by spectral data that unfolded molecules in the refolding condition assume a new conformation different from that of unfolded molecules in the initial unfolding condition. The spectral properties for the unfolded molecule, which exists only transiently in the refolding process, could be measured from the total amplitude of the refolding kinetics. The molar absorbance for the unfolded molecule in the initial unfolding condition was measured by difference spectroscopy. For both measurements the native molecule in the final condition was used as a reference.

The rapid kinetic and static data, both obtained in the stopped-flow apparatus, are compared in Figure 5. For a reasonable comparison, the static data should be corrected for the solvent effect. In other words, we need to estimate the absorbance difference expected for the hypothetical situation that the denatured protein molecules exist in the refolding condition in the same conformation as in the initial unfolding condition. The required data, the change in molar absorbance with denaturant concentration, were measured in a Hitachi 320 recording spectrophotometer. The results are shown in Figure 6 for GdmCl-induced denaturation and in Figure 7 for HOAc-induced denaturation. The change in difference absorbance with denaturant concentration in the post-transition region was fitted by a straight line, which was then extrapolated to the final refolding condition to estimate the absorbance difference corrected for the solvent effect. The ratio of the corrected and uncorrected values thus obtained was multiplied

Table I: Kinetic Parameters for the Refolding of HEWL at 25 °C[a]

initial conditions	final conditions	wavelength (nm)	τ_2 (s)	τ_1 (s)	A_2 (M^{-1} cm^{-1})	A_2 (M^{-1} cm^{-1})	$A_2/(A_1 + A_2)$
4 M GdmCl, pH 2.5	0.5 M GdmCl, pH 2.6	301	1.3	16	+1350	+160	0.89
		292	1.1	19	−1090	−120	0.90
		250	1.3	18	−2120	−230	0.90
40% HOAc, pH 1.8	5% HOAc, pH 2.6	301	0.15	3.5	+1250	+120	0.91
		292	0.15	3.3	−1630	−150	0.92
		250	0.15	1.7	−2200	−200	0.92
4 M GdmCl, pH 2.5	0.5 M GdmCl and 5% HOAc, pH 2.4	301	2.6	21	+1130	+220	0.84
		292	2.5	24	−1360	−230	0.86
		250	2.7	25	−2000	−340	0.85
40% HOAc, pH 1.8	0.5 M GdmCl and 5% HOAc, pH 2.4	301	2.5	15	+1160	+170	0.87
		292	2.5	22	−1300	−230	0.85
		250	2.5	23	−1990	−350	0.85

[a] The initial and final conditions with GdmCl contained 0.05 M glycine-HCl buffer, pH 2.6. The final protein concentrations were 0.4 mg/mL. The positive and negative signs of the amplitude indicate that the absorbance was decreasing and increasing, respectively, in the refolding process.

by the static data obtained in the stopped-flow apparatus. The hatched bars in Figure 5 show the results.

For the absorbance difference at 301 nm, the static result approaches the kinetic result after the correction is made. However, at the other two wavelengths, the difference between the static result and the kinetic result is increased by the correction. We conclude, therefore, that unfolded HEWL, being present transiently after refolding is initiated, has a conformation different from that in the initial denatured solution according to its absorption spectrum. The same conclusion may be drawn for the refolding conditions containing both denaturants, although the data corrected for the solvent effect are not available at hand.

Discussion

We have shown in the present study that the kinetics of HEWL refolding outside the transition region are biphasic and that the kinetic parameters are independent of the wavelength of light used for observation. Our data, therefore, have resolved a discrepancy contained in the work of Tanford et al. (1973). The biphasic refolding kinetics at higher GdmCl concentrations and the uniphasic unfolding kinetics outside the transition region (S. Kato et al., unpublished data) suggest that the folding kinetics of HEWL may also be interpreted in terms of the three-species model $U_1 \rightleftharpoons U_2 \rightleftharpoons N$ as in RNase A. The interconversion between the two unfolded species has been interpreted as the cis–trans isomerization of the proline residues (Brandts et al., 1975). The experimental evidence supporting the view is increasing (Brandts et al., 1977; Lin & Brandts, 1978; Schmid & Baldwin, 1978; Stellwagen, 1979). In our data a higher fraction of total amplitude occurs in the fast phase than predicted by the theory, 0.64, for the protein (HEWL) containing two proline residues in the trans configuration. This fraction depends somewhat on the GdmCl concentration in the final condition (data not shown). Perhaps these results should not be taken simply as evidence against the proline isomerization model for the reasons (1) the presence of certain "permissive" proline residues has been suggested, (2) the cis–trans equilibrium constant depended on contributions by the bulkiness of the side chains adjacent to the proline residues, on preferential intra- and interpeptide interactions, and on the nature of the solvent [recent discussion by Stellwagen (1979)].

The use of two denaturants, GdmCl and HOAc, in the present study permits refolding experiments in the same final condition starting from different initial conditions. The results unequivocally show that the refolding kinetics depends only on the final refolding condition. Nall et al. (1978) reported a second slower refolding process in the refolding of pH-unfolded RNase A, whose amount depended on the GdmCl concentration in the initial unfolding condition. This reaction may be due to some aggregates as suggested in the original paper. One thing to which we should pay close attention in using concentrated acetic acid is to avoid the irreversible damage of proteins, presumably by deamidation (Manjula et al., 1976).

We have shown here quantitatively that the total kinetic amplitude of refolding, obtained with the rapid stopped-flow method, differs from the absorbance difference between the equilibrium values in the initial unfolded state and in the final refolding state. This conclusion remains valid when a correction for the solvent effect is made. Thus the unfolded species in the refolding condition takes a new conformation defined by the final refolding condition. The transformation between the two conformations, in the initial unfolding and in the final refolding conditions, was completed within the dead time of the stopped-flow apparatus. We have thus detected an intermediate that exists in the refolding kinetics of HEWL. As further evidence for the fast transformation, the change of the HEWL conformation between the two unfolded states, 4 M GdmCl and 40% HOAc, was too fast to be detected by the stopped-flow measurements at 301 nm, where the difference in the absorbance value is large (data not shown). This indicates that the conformational change is associated with only short-range interactions. The denaturant molecules preferentially bound to the unfolded species may affect the secondary structure. It is unlikely, however, that the secondary structure is the same as that in the native compact conformation. The denatured species in the refolding condition will be essentially in the extended conformation. The native tertiary structure will be produced as a result of cooperative long-range interactions between microdomains as in the diffusion-collision model of Karplus & Weaver (1976). This view may be supported by the recent result of Creighton (1979) that a unique folding route was not found for RNase A by trapping disulfide intermediates.

Recently, Schmid & Baldwin (1979) made a refolding kinetic study with use of the unfolded RNAse A whose exchangeable amide protons were labeled with ^3H. They detected an early protection of amide protons preceding the folding of the overall tertiary structure. Thus a structural intermediate was found both for RNase A and HEWL by two different experimental approaches.

The difference between the kinetic and static amplitudes for refolding gives two important suggestions for refolding experiments: (1) The kinetic reversibility should be checked

not only by spectra but also by the recovery of enzymatic activity. The complete (100%) recovery of enzymatic activity was confirmed for the refolded protein in the present study (data not shown). (2) The complete unfolding of proteins in the initial condition, with use of GdmCl at high concentration (Tanford, 1968), may not always be necessary, because the unfolded molecules may anyway take a specific secondary structure characteristic of the refolding condition before the molecules start refolding.

Acknowledgments

We thank Robert L. Baldwin for critical reading of the manuscript and for valuable suggestions.

References

Baldwin, R. L. (1975) *Annu. Rev. Biochem. 44*, 453–475.
Baldwin, R. L. (1978) *Trends Biochem. Sci. 3*, 66–68.
Brandts, J. F., Halvorson, H. R., & Brennen, M. (1975) *Biochemistry 14*, 4953–4963.
Brandts, J. F., Brennen, M., & Lin, L.-N. (1977) *Proc. Natl. Acad. Sci. U.S.A. 74*, 4178–4181.
Canfield, R., & Liu, A. K. (1965) *J. Biol. Chem. 240*, 1977–2002.
Creighton, T. E. (1979) *J. Mol. Biol. 129*, 411–431.
Garel, J.-R., & Baldwin, R. L. (1973) *Proc. Natl. Acad. Sci. U.S.A. 70*, 3347–3351.
Garel, J.-R., & Baldwin, R. L. (1975a) *J. Mol. Biol. 94*, 611–620.
Garel, J.-R., & Baldwin, R. L. (1975b) *J. Mol. Biol. 94*, 621–632.
Hagerman, P. J. (1977) *Biochemistry 16*, 731–747.
Hagerman, P. J., & Baldwin, R. L. (1976) *Biochemistry 15*, 1462–1473.
Hammes, G. G., & Roberts, P. B. (1969) *J. Am. Chem. Soc. 91*, 1812–1816.
Hiromi, K., Ono, S., & Nagamura, T. (1968) *J. Biochem. (Tokyo) 64*, 897–900.
Karplus, M., & Weaver, D. C. (1976) *Nature (London) 260*, 404–406.
Lin, L.-N., & Brandts, J. F. (1978) *Biochemistry 17*, 4102–4181.
Manjula, B. N., Acharya, A. S., & Vithayathil, P. J. (1976) *Int. J. Protein Res. 8*, 275–282.
Nall, B. T., Garel, J.-R., & Baldwin, R. L. (1978) *J. Mol. Biol. 118*, 317–330.
Nozaki, Y. (1972) *Methods Enzymol. 26*, 43–50.
Schmid, F. X., & Baldwin, R. L. (1978) *Proc. Natl. Acad. Sci. U.S.A. 75*, 4764–4768.
Schmid, F. X., & Baldwin, R. L. (1979) *J. Mol. Biol. 135*, 199–215.
Schwarz, G. (1965) *J. Mol. Biol. 11*, 64–77.
Sophianopoulos, A. J., Rhodes, C. K., Holcomb, D. N., & Van Holde, K. E. (1962) *J. Biol. Chem. 237*, 1107–1112.
Stellwagen, E. (1979) *J. Mol. Biol. 135*, 217–229.
Tanford, C. (1968) *Adv. Protein Chem. 23*, 121–282.
Tanford, C., Aune, K. C., & Ikai, A. (1973) *J. Mol. Biol. 24*, 189–197.
Tonomura, B., Nakatani, H., Onishi, M., Yamaguchi-Ito, J., & Hiromi, K. (1978) *Anal. Biochem. 84*, 370–383.
Wetlaufer, D. B., Johnson, E. R., & Clauss, L. M. (1974) in *Lysozyme* (Osserman, E. F., Canfield, R. E., & Beychok, S., Eds.) pp 269–280, Academic Press, New York.

Information Content in the Circular Dichroism of Proteins†

John P. Hennessey, Jr., and W. Curtis Johnson, Jr.*

ABSTRACT: A method is presented for predicting the secondary structure of a protein from its circular dichroism (CD) spectrum. Eight types of secondary structure are considered: helix; parallel and antiparallel β strand; types I, II, and III β turn; all other β turns combined; and "other" structures. The method is based on mathematical calculation of orthogonal basis CD spectra from the CD spectra of proteins with known secondary structure. Five basis CD spectra are needed to reconstruct the 16 original protein CD spectra that extend into the vacuum ultraviolet region to 178 nm. Thus, one can expect to extract five independent pieces of information from the CD spectrum of a protein. Each basis CD spectrum corresponds to a known mixture of secondary structures so that the coefficients that reconstruct the protein CD spectrum can also be used to predict secondary structure. Furthermore, when the same method is applied to protein secondary structure rather than CD, it is found that only five basis secondary structure vectors are needed to reconstruct the original protein secondary structure vectors. Thus there are five independent "superstructures", consisting of a mixture of standard secondary structures, in the proteins studied. It would appear that there is enough information in the CD spectrum of a protein to predict all types of secondary structure. Our CD analyses compare favorably with the X-ray data.

It is generally accepted that the circular dichroism (CD)[1] spectrum of a protein is a direct reflection of its secondary structure. Over the past 15 years attempts have been made to correlate the two by using a variety of theoretical and empirical techniques, all finding various degrees of success. Use of CD spectra of polypeptides, in theoretically known structural conformations, as basis spectra has been one of the foremost techniques (Greenfield et al., 1967; Greenfield &

† From the Department of Biochemistry and Biophysics, Oregon State University, Corvallis, Oregon 97331. *Received August 5, 1980.* This work was supported by National Science Foundation Grant PCM76-81556 from the Biophysics Program, National Institutes of Health Biomedical Research Support Grant RR07079, and a grant from the Oregon State University Computer Center.

[1] Abbreviations used: CD, circular dichroism; vacuum UV, vacuum ultraviolet; H, helix; A, antiparallel β strand; P, parallel β strand; I, type I β turn; II, type II β turn; III, type III β turn; T, remaining types of β turn combined; O, "other" structure; *r*, correlation coefficient; rms, root mean square.

0006-2960/81/0420-1085$01.25/0